Published in final edited form as:
Int J Pharm. 2014 October 20; 474(0): 14–24. doi:10.1016/j.ijpharm.2014.07.056.

MOLECULAR EXPRESSION AND FUNCTIONAL ACTIVITY OF VITAMIN C SPECIFIC TRANSPORT SYSTEM (SVCT2) IN HUMAN BREAST CANCER CELLS

Varun Khurana[1,2], **Deep Kwatra**[1,3], **Dhananjay Pal**[1], and **Ashim K. Mitra**[1]

[1]Division of Pharmaceutical Sciences, School of Pharmacy, University of Missouri-Kansas City, 2464 Charlotte Street, Kansas City, MO 64108-2718, USA

[2]INSYS Therapeutics Inc, 444 South Ellis Road, Chandler, AZ 85224, USA

[3]Department of Molecular and Integrative Physiology, University of Kansas Medical Center, Kansas City, Kansas, 66160, USA

Abstract

The main goal of this study is to investigate the expression of sodium dependent vitamin C transport system (SVCT2). Moreover this investigation has been carried out to define uptake mechanism and intracellular regulation of ascorbic acid (AA) in human breast cancer cells (MDA-MB231, T47D and ZR-75-1). Uptake of [^{14}C] AA was studied in MDA-MB231, T47D and ZR-75-1 cells. Functional parameters of [^{14}C] AA uptake were delineated in the presence of different concentrations of unlabeled AA, pH, temperature, metabolic inhibitors, substrates and structural analogs. Molecular identification of SVCT2 was carried out with reverse transcription–polymerase chain reaction (RT-PCR). Uptake of [^{14}C] AA was studied and found to be sodium, chloride, temperature, pH and energy dependent in all breast cancer cell lines. [^{14}C] AA uptake was found to be saturable, with K_m values of 53.85±6.24, 49.69±2.83 and 45.44±3.16 μM and V_{max} values of 18.45±0.50, 32.50±0.43 and 33.25±0.53 pmol/min/mg protein, across MDA-MB231, T47D and ZR-75-1, respectively. The process is inhibited by structural analogs (L-AA and D-Iso AA) but not by structurally unrelated substrates (glucose and PAHA). Ca^{++}/calmodulin and protein kinase pathways appeared to play a crucial role in modulating AA uptake. A 626 bp band corresponding to a vitamin C transporter (SVCT2) based on the primer design was detected by RT-PCR analysis in all breast cancer cell lines. This research article describes AA uptake mechanism, kinetics, and regulation by sodium dependent vitamin C transporter (SVCT2) in MDA-MB231, T47D and ZR-75-1 cells. Also, MDA-MB231, T47D and ZR-75-1 cell lines can be

*Corresponding author: Ashim K. Mitra, Ph.D., Curators' Professor and Chairman, Division of Pharmaceutical Sciences, School of Pharmacy, University of Missouri-Kansas City, 2464 Charlotte Street, Kansas City, MO 64108, USA, Phone: 1-816-235-1615, Fax: 1-816-235-5190, mitraa@umkc.edu.

Author Disclosure Statement
No competing nancial interests exist.

utilized as a valuable *in vitro* model to investigate absorption and permeability of AA-conjugated chemotherapeutics.

Keywords

Ascorbic acid kinetics; targeted drug delivery; *in vitro* cell culture models; MDA-MB231; T47D and ZR-75-1 cells; nutrient transporter

1. Introduction

In United States, 1 in 8 women develop breast cancer during their lifespan. In 2013 about 232,340 new cases of breast cancer were diagnosed among American women. Breast cancer represents 14.1% of all new cancer cases in the U.S (cancer.gov-recent statistics). Although, chemotherapy has shown promising results in treating breast cancer, it frequently leads to systemic side effects. Also, acquired drug resistance has been reported due to the frequent use of multiple chemotherapeutic drugs during treatment of advanced breast cancer (Doyle et al., 1998; Stebbing and Ellis, 2012). During lactating period, breast epithelial cells are responsible for transport of amino acids and vitamins across cell membranes in order to meet the requirements of accelerated milk-protein synthesis. However, information is still limited with respect to transport of amino acids and vitamins across breast epithelial cells and its regulation in various biological and pathological progressions (Bareford et al., 2008) (Shennan, 1998; Vadlapudi et al., 2013). Presence of efflux transporter proteins i.e., P-glycoprotein (P-gp or MDR1), multidrug resistance proteins (MRPs) and breast cancer resistance protein (BCRP) render drug delivery to the breast cancer cells at therapeutic doses highly challenging (Cole et al., 1992; Doyle et al., 1998; Gros et al., 1986; Kessel et al., 1968; Ling and Thompson, 1974; Riehm and Biedler; Vadlapudi et al., 2013). In cancer patients, overcoming multidrug resistance by exploring strategies such as evasion or modulation of these efflux transporters may play a vital role (Khurana et al., 2014a; Khurana et al., 2014b; Minocha et al.; Vadlapudi et al., 2013). Several reports suggested high level expressions of influx/nutrient transporters, such as biotin (Vadlapudi et al., 2013), nucleoside/nucleobase (Marshman et al., 2001; Plagemann et al., 1988), glucose (Rivenzon-Segal et al., 2000), monocarboxylic acid (Gallagher et al., 2007; Harris et al., 2009), folate (Jhaveri et al., 2004; Pinard et al., 1996), organic anion and cation transporters (Okabe et al., 2008) on various breast cancer cells. This information, in turn, facilitates the rational design of novel anti-cancer therapeutic targeting a specific carrier mediated transporter expressed in breast cancer cells (Tamai, 2012).

Ascorbic acid (AA, vitamin C) is an essential water-soluble vitamin required for physiological and metabolic functions. It is an important nutrient required as a cofactor by various metabolic enzymes (Hong et al., 2013; Menniti et al., 1986; Murad et al., 1981; Patak et al., 2004). Efficacy of AA in cancer treatment has a controversial history (Hong et al., 2013; Padayatty and Levine, 2000). Many published reports described beneficial effects of AA in cancer treatment. AA has shown inhibitory effects on various cancer cells including breast, brain, prostate and stomach (Baader et al., 1996; Head, 1998; Hong et al., 2013; Kang et al., 2005; Maramag et al., 1997). Also, pharmacologic doses of AA, 10 g daily, showed effective results in the average survival of advanced cancer patients, improved

patient well-being and reduced pain (Cameron and Campbell, 1974; Cameron and Pauling, 1976; Cameron and Pauling, 1978; Hong et al., 2013; Ohno et al., 2009). In human breast carcinoma cells, AA appears to potentiate the antineoplastic activity of doxorubicin, cisplatin, and paclitaxel (Kurbacher et al., 1996). AA plays an important role in enhancing natural immunity and may cause lowest toxicity of all the vitamins (Ohno et al., 2009).

AA cannot be synthesized by human and other primates, thus making this vitamin an essential dietary requirement. Therefore, AA is usually obtained from exogenous sources through the dietary intake (Luo et al., 2008). AA uptake via specific transport system has already been reported in intestine (Maulen et al., 2003), brain (Castro et al., 2001), kidney (Bowers-Komro and McCormick, 1991), skin (Padh and Aleo, 1987), eye (Garland, 1991; Talluri et al., 2006) and bone (Dixon et al., 1991). Human *SLC23A2* family consists of two isoforms of sodium-dependent vitamin C transporters (SVCT) namely SVCT1 and SVCT2 (Burzle et al., 2013). A relative study of two isoforms discloses that AA exhibits higher structural and functional tropisms towards SVCT2 than SVCT1. Both SVCT1 and SVCT2 vary in distribution but express close sequence homology and functional similarity (Talluri et al., 2006). Structural and functional studies reveal that transport of AA across epithelial cells is primarily facilitated via SVCT (Luo et al., 2008; Talluri et al., 2006).

Transporter targeted drug delivery, in recent years, has been widely explored to improve targeted drug delivery across biological membranes. An active agent is chemically modified with transporter targeted moieties, this bioreversible conjugate enhances drug permeation and absorption. Facilitated transport of conjugated drug interacts with targeting moiety and the transporter resulting in elevated absorption (Patel et al., 2012). SVCT2 has been exploited by many investigators as an important target for drug delivery across epithelial membranes. Higher absorptive permeability and metabolic stability compared to saquinavir alone has been observed with AA conjugated saquinavir (Luo et al., 2011). Conjugation of nipecotic, kynurenic and diclophenamic acids with AA has been employed to enhance transport of therapeutic agents. This approach has provided a new perspective for transporter/receptor targeted prodrug design targeted to SVCT2 transporter (Manfredini et al., 2002). Hence, SVCT targeted drug delivery can be utilized as a vital strategy for enhancing intracellular accumulation of anti-cancer in cancer cells. The aim of this study is to investigate the expression of a specialized carrier mediated transport system (SVCT2) on the epithelia of breast cancer cells (MDA-MB231, T47D and ZR-75-1).

The presence of SVCT on corneal cells and Madin-Darby canine kidney cells has been previously reported from our laboratory (Luo et al., 2008; Talluri et al., 2006). Also, SVCT expression was shown on breast cancer epithelial cells (MDA-MB231 and T47D cells). However, no information currently exists regarding mechanistic and functional processes as well as molecular expression of AA carrier mediated uptake by breast cancer cells. In the present study, we evaluated the ascorbic acid uptake process, kinetics as well as expression, relative contribution, and regulation of SVCT2 in MDA-MB231, T47D and ZR-75-1 cells. Results obtained from this study may indicate involvement of a specific and high affinity carrier transport system (SVCT2) for translocation of AA.

2. Material and methods

2.1. Materials

[^{14}C] Ascorbic acid ([^{14}C] AA specific activity 8.5 mCi/mM) was procured from Perkin Elmer (Boston, MA, USA). Unlabeled L-ascorbic acid, D-iso-ascorbic acid, dehydro-ascorbic acid (DHAA), glucose, para amino hippuric acid (PAHA), sodium azide, ouabain, 2,4-dinitrophenol, choline chloride, HEPES, bovine insulin, human epidermal growth factor, Triton X-100, phorbol-12-myristate-13-acetate (PMA), bisindolylmaleimide I (BIS), 3-isobutyl-1-methylxanthine (IBMX), 4,4′-di-isothiocyanatostilbene- 2,2′-disulphonic acid (DIDS), 4-acetamido-4′-isothiocyanostilbene-2,2′-disulfonic acid (SITC), and D-glucose were purchased from Sigma Chemical Co (St. Louis, MO, USA). Culture media (Dulbecco's modified Eagle's medium (DMEM), RPMI 1640 culture medium and DMEM/F-12) were procured from Invitrogen (Carlsbad, CA, USA). Fetal bovine serum (FBS) was obtained from Atlanta biologicals (Lawrenceville, GA, USA). Culture flasks (75 cm^2 growth area) and uptake plates (3.8 cm^2 growth area) were purchased from Corning Costar Corp. (Cambridge, MA, USA). The buffers for cDNA synthesis and amplification (oligodT, dNTP, MgCl2, M-MLV reverse transcriptase and Taq polymerase) were obtained from Promega Corporation (Madison, WI, USA). Light Cycler 480® SYBR I green master mix was obtained from Roche Applied Science (Indianapolis, IN, USA). Qualitative and quantitative primers used in the study were custom-designed and obtained from Invitrogen Life Technologies (Carlsbad, CA, USA). All other chemicals were obtained from Fisher Scientific Co. (Fair Lawn, NJ, USA) and utilized without further purification.

2.2. Cell Culture

T47D cells were obtained from American Type Culture Collection (ATCC). MDA-MB-231 and ZR-75-1 cells were generous gifts from Dr. Walter Jäger University of Vienna, Austria) and Dr. A.J. van Agthoven (Josephine Nefkens Institute, Netherlands), respectively. T47D cells were cultured according to a previously published protocol (Vadlapudi et al., 2013). Cells of passage numbers between 20 and 30 were cultured at 37°C, humidified 5% CO_2/95% air atmosphere in a DMEM culture medium supplemented with 10% (v/v) FBS (heat inactivated), 1% nonessential amino acids, 20 mM HEPES, 29 mM sodium bicarbonate, 100 mg of penicillin and streptomycin.

ZR-75-1 cells were cultured at 37°C, humidified 5% CO_2/95% air atmosphere in a RPMI 1640 culture medium supplemented with 10% (v/v) FBS (heat inactivated), 29 mM $NaHCO_3$, 20 mM HEPES, 100 mg of penicillin and streptomycin each, and 1 nM estradiol. (0.5 ml/500 ml medium) at pH 7.4 (Constable et al., 2006; Davis et al., 1995). The growth medium was changed every alternate day.

MDA-MB-231 cells were cultured at 37°C, humidified 5% CO_2/95% air atmosphere in a DMEM/F12 culture medium supplemented with 10% (v/v) FBS, 29 mM $NaHCO_3$, 20 mM HEPES, 100 mg of penicillin and streptomycin each.

All breast cancer cell lines were cultured in 75 cm^2 flasks, harvested at 80–90% confluency with TrypLE™ Express (Invitrogen, Carlsbad, CA, USA). Cells were then plated in 24-well

uptake plates at a density of 300,000 cells/well. Cells were grown in a similar way as mentioned above and utilized for additional studies.

2.3. Uptake Studies

Confluent breast cancer cells were employed for uptake experiments. Following media removal, cells were rinsed thrice for 5 min each with 1–2 ml of Dulbecco's phosphate-buffered saline (DPBS) containing 140 mM NaCl, 0.03 mM KCl, 7.5 mM Na_2HPO_4, 1.5 mM KH_2PO_4, 1 mM $CaCl_2$, 0.5 mM $MgSO_4$, 20 mM HEPES, and 5 mM glucose maintained at pH 7.4. Uptake studies were initiated by adding 250μl of solution containing 0.25 μCi/ml of [^{14}C] AA in the presence and absence of various competing substrates. Following specific period of incubation, the solution was removed and uptake process was terminated with 2 ml of ice-cold stop solution containing 200 mM KCl and 2 mM HEPES. The cell monolayer was washed thrice, 5 min each and 1ml of lysis buffer (0.1% Triton-X solution in 0.3% NaOH) was added to each well and plates were stored overnight at room temperature. Subsequently, the cell lysate (400μl) from each well was transferred to scintillation vials containing 3 ml of scintillation cocktail (Fisher Scientific, Fairlawn, NJ, USA). Samples were quantified by measuring the radioactivity using liquid scintillation spectrophotometer coulter (Beckman Instruments Inc., Fullerton, CA, USA, model LS-6500). Protein content of each sample was estimated by BioRad Protein Estimation Kit (BioRad Protein Estimation Kit, Hercules, CA, USA).

2.3.1. Time and temperature dependency—The optimum time for uptake studies of [^{14}C] AA were determined by performing the uptake studies over various time points (5, 10, 15, 30, 45 and 60 min). The uptake study was conducted as per method described earlier. The effect of temperature on [^{14}C] AA uptake was determined by carrying out the uptake study at different temperatures i.e. 4°C, 25°C and 37°C. The buffer temperature was adjusted to 4°C, 25°C and 37°C prior to the initiation of [^{14}C] AA uptake.

2.3.2. pH and ion dependency—The effect of pH on [^{14}C] AA uptake was observed by adjusting the pH to 5, 6, 6.5, 7.4 and 8. For delineating the role of sodium ions on [^{14}C] AA uptake, sodium chloride (NaCl) and sodium phosphate dibasic (Na_2HPO_4) in DPBS were substituted with equimolar quantities of choline chloride and potassium phosphate dibasic (KH_2PO_4), respectively. Hill coefficient for uptake of AA as function of Na^+ was determined. In a similar manner, buffer solution containing sodium (140 mM), potassium (0.03 mM), and calcium (1 mM) chlorides were replaced with equimolar quantities of sodium phosphate, potassium phosphate, and calcium acetate, respectively.

In another study, cells were pre-incubated with 1 mM amiloride (sodium channel inhibitor) and the uptake study was carried out as mentioned earlier.

2.3.3. Concentration dependency—Several concentrations of L-AA were prepared ranging from (0.12–2000μM) in DPBS (pH 7.4) and spiked with [^{14}C] AA (0.25μCi/ml). The uptake studies were performed according to a previously described method (Vadlapudi et al., 2013). The data was fitted to Michaelis-Menten equation as shown in section 3.2 and

the maximum transport rate (V_{max}) and Michaelis-Menten constant (K_m) were calculated according to nonlinear least squares regression analysis program; GraphPad Prism version 5.

2.3.4. Role of metabolic and membrane transport inhibitors—For energy dependency studies, simultaneous incubation of [^{14}C] AA along with metabolic inhibitors such as ouabain (Na^+/K^+ ATPase inhibitor), 2,4-dinitrophenol (intracellular ATP reducer) and sodium azide (oxidative phosphorylation inhibitor) were performed for 1h. In order to examine the effect of anionic membrane transport inhibitors, cells were pre-incubated with 1mM SITC, DIDS and probenecid for 1h.

2.3.5. Substrate specificity—The substrate specificity for SVCT was delineated by carrying out [^{14}C] AA uptake in the presence of three concentrations of (500, 1000 and 2000μM) unlabeled L-AA and structural analogs such as D-Iso AA and DHAA. A similar study was carried out at three different concentrations of (500, 1000 and 2000μM) of various structurally unrelated analogs such as glucose (Glucose transporter/GLUT substrate) and PAHA (organic anion transporter/OAT substrate).

2.3.6. Intracellular regulation—Involvement of various intracellular regulatory pathways such as Ca^{++}/calmodulin, PTK (protein tyrosine kinase), PKC (protein kinase C) and PKA (protein kinase A) pathway on [^{14}C] AA uptake was also investigated. Cells were pre-incubated with modulators such as calmidazolium (CaM) and KN-62 to delineate the process. In order to examine the role of PTK pathway in [^{14}C] AA uptake, cells were pre-incubated with genistin and tyrphostin A25. For studying the effect of PKC pathway, cells were pre-incubated with BIS and PMA (modulators of PKC pathway). The effect of PKA pathway was studied by incubating the cells with IBMX and forskolin (modulators of PKA pathway). Uptake of [^{14}C] AA was then performed according to the procedure as previously described.

2.3.7. Reverse Transcription–Polymerase Chain Reaction—Reverse transcription–polymerase chain reaction (RT-PCR) analysis was carried out to determine the expression of SVCT2 on T47D, MDA-MD-231 and ZR-75-1 at molecular level. TRIzol® reagent (Invitrogen, USA) was used to perform cell lysis. Chloroform was added to the lysate for phase separation. Following separation of aqueous phase containing RNA, isopropanol was added to precipitate RNA which was rinsed twice with 75% ethanol followed by resuspension in RNase-DNase free water. The concentration and purity of RNA was determined with Nanodrop (Thermo Fisher Scientific, Wilmington, DE, USA). RNA was reverse-transcribed to obtain cDNA using oligodT as a template and M-MLV reverse transcriptase. The conditions for reverse transcription were: denaturation of the template RNA for 5 min at 70°C; reverse transcription for 60 min at 42°C followed by final extension at 72°C for 5 min. cDNA obtained was then subjected to PCR for amplification of SVCT using specific set of primers. Set of primers (5′→3′) designed for SVCT2 were: forward: CCAGCGGTGAGCAGGACAAT, reverse primer: TAGGGCCACCGTGGGTGTAA. These primers correspond to a 626 base pair (bp) product in human SVCT2 cDNA. β-Actin was used as internal standard and primers used were: forward: AACCGCGAGAAGATGACCCAGATCATGTTT. Reverse primer:

AGCAGCCGTGGCCATCTCTTGCTCGAAGTC. These primers correspond to a 351 base pair (bp) product in human β-Actin cDNA. The conditions of PCR amplification were: denaturation for 30 s at 94°C, annealing for 1 min at 56°C, and extension for 1 min at 72°C, for 45 cycles followed by a final extension for 5 min at 72°C. PCR product obtained was analyzed by gel electrophoresis on 1.5% agarose in TAE buffer and visualized under UV (Vadlapudi et al., 2012). The real time PCR for each sample was done in triplicates and three different batches of cells were tested to ensure reproducibility and to eliminate bath to batch variation.

2.3.8. Quantitative Real-Time PCR—Following reverse transcription, quantitative real-time PCR (qPCR) was performed with LightCycler® SYBR green technology (Roche). cDNA equivalent to 80 ng in each well was subjected to amplification with specific primers. Glyceraldehyde-3-phosphate dehydrogenase (GAPDH) was used as an internal standard to normalize the amount of cDNA in each well. The sequences of real-time primers (5′→3′) used for SVCT2 were: forward: GCCAGCTAGGTCTTGACTCC, reverse primer: GATGTGGCGTAGACCTGTCC, GAPDH: forward—ATCCCTCCAAAATCAAGTGG and reverse—GTTGTCATGGATGACCTTGG. A preliminary experiment was performed to ensure that SVCT2 and GAPDH were amplified with equal efficiencies. The specificity of these primers was also confirmed by melting-curve analysis. The comparative threshold method was used to calculate the relative amount of SVCT2 in breast cancer cell lines (Pfaffl, 2001; Vadlapudi et al., 2012).

3. Data Analysis

3.1. Radioactive Sample Analysis

The uptake of [^{14}C] AA was calculated using disintegrations per minute (DPM) of sample and donor solutions as shown in Eq. 1

$$Csample = \frac{DPMsample * Cdonor}{DPMdonor} \quad \text{Eq. 1}$$

where, DPM_{sample} and DPM_{donor} represent average values of DPM counts of sample and donor (n=4) respectively; C_{donor} denotes the concentration of donor used and C_{sample} represents the concentration of sample.

3.2. Calculation of Michaelis-Menten Kinetic Parameters

In order to determine K_m and V_{max} associated with [^{14}C] AA uptake, concentration-dependency data was fitted in a modified Michaelis–Menten equation as shown in Eq.2

$$v = \frac{Vmax[C]}{Km + [C]} + Kd[C] \quad \text{Eq. 2}$$

v represents the total uptake, V_{max} stands for the maximum uptake rate for the carrier-mediated process, K_m is Michaelis–Menten constant which represents the concentration at half saturation, K_d is a non-saturable diffusion rate constant and C is substrate concentration.

In Eq. (2), (V_{max}*C)/(K_m+C) represents carrier mediated saturable process whereas K_d(C) denotes the non-saturable component. Data was fitted to a non-linear least-square regression analysis program (GraphPad Prism 5.0). The Michaelis-Menten kinetic parameters were calculated to determine saturable and non-saturable component of the total uptake.

3.3. Calculation of Hill Ratio

Na^+:L-Ascorbic acid coupling ratio was determined using the logarithmic form of the Hill equation (Eq. 3)

$$Log\left[\frac{v'}{Vmax}-v'\right]=nlog(S)-logK' \quad \text{Eq. 3}$$

v′ denotes initial velocity, V_{max} represents the maximal velocity, n is number of substrate binding sites, S denotes the substrate concentration, and K′ is a constant comprising multiple interaction factors and the intrinsic dissociation constant.

3.4. Statistical Analysis

All the experiments were conducted at least in quadruplicate (n=4) and the outcomes were expressed as mean±standard deviation (SD). To calculate statistical significance, Student T-test or one way ANOVA with Tukey's post hoc test has been utilized in the manuscript for analysis as per requirement and the difference between mean values is considered statistically significant for P value ≤0.05.

4. Results

4.1. Time and temperature dependency

Time dependent uptake of [^{14}C] AA in MDA-MB231, T47D and ZR-75-1 cells is depicted in Fig. 1. Linear uptake of [^{14}C] AA was noticed upto 60 min of incubation period. Therefore, 30 min uptake time was selected for all uptake experiments.

Effect of temperature on the uptake of AA was studied on MDA-MB231, T47D and ZR-75-1 cells. Uptake of [^{14}C] AA in the three breast cancer cell lines was maximal at 37°C (Fig. 2). Uptake of [^{14}C] AA in MDA-MB231 showed ~40% and 70% decrease when the temperature was reduced to 25°C and 4°C respectively. In T47D cells, uptake was reduced to ~55% and 25% when measured at 25°C and 4°C respectively, whereas, in ZR-75-1 cells uptake of [^{14}C] AA diminished to ~50% and 20% respectively, at 25°C and 4°C, suggesting that the process may be carrier mediated in all the studied breast cancer cell lines. Activation energy (E_a) was calculated by plotting the temperature dependent data i.e. Uptake rate Ln(v) vs. 1/T (Fig. 3) E_a was calculated to be 8.08, 9.71 and 9.99 kcal/mol in MDA-MB231, T47D and ZR-75-1 cells respectively.

4.2. pH and ion dependency

In order to delineate the role of an inward driven proton gradient for [^{14}C] AA uptake, the study was carried out with pH ranging from 5–8 in MDA-MB231, T47D and ZR-75-1 cells. Uptake of [^{14}C] AA elevated with a rise in extracellular pH from 5 to 8 in all cell lines. In

comparison to pH 7.4, uptake of [^{14}C] AA diminished to ~40% and 50% at pH 5 and 6 respectively in MDA-MB231, T47D and ZR-75-1 cells (Fig. 4). Based on these results, further uptake studies were carried out at pH 7.4 with all the cell lines.

In sodium free media, uptake of [^{14}C] AA was reduced to ~50%, 25% and 30% respectively, in MDA-MB231, T47D and ZR-75-1 cells (Fig. 5A). Similarly, uptake of AA was also diminished to ~%60, 50% and 50% in MDA-MB231, T47D and ZR-75-1 cells respectively in the presence of amiloride (Na^+ transport inhibitor), indicating possible involvement of sodium ions in translocation of AA (Fig. 5A).

The effect of chloride ions was studied by replacing chloride ions with equimolar quantities of other monovalent cations in DPBS. A marked reduction (45%, 40% and 40%) in the uptake rate of [^{14}C] AA was observed in the absence of chloride ions in MDA-MB231, T47D and ZR-75-1 cells respectively. This study evidently defines the involvement of sodium and chloride ions in active transport of AA (Fig. 5A).

Role of sodium on AA absorption kinetics of AA was also evaluated with various concentrations of sodium (0–140mM) in the DPBS. Reduced uptake of [^{14}C] AA was observed with lower Na^+ concentrations. Uptake data displayed saturation kinetics of [^{14}C] AA uptake at about 70 mM of Na^+ concentration in MDA-MB231, T47D and ZR-75-1 cells (Fig. 5B). Hill transformation of Na^+ saturation kinetics data showed 2:1 molar ratio of Na^+:AA coupling in these breast cancer cell lines (Fig. 6).

4.3. Concentration dependency

Breast cancer cells were incubated with various concentrations (0.12–2000μM) of unlabeled AA for 30 min at 37°C, in order to investigate Michaelis-Menten saturation kinetics. The uptake process involves both the saturable carrier mediated pathway and non-saturable diffusional process in all three breast cancer cell lines. Uptake of [^{14}C] AA was reduced at 4°C compared to 37°C indicating the role of passive diffusion component involved in AA transport in breast cancer cells. The carrier mediated process of AA uptake in breast cancer cell lines was plotted as the difference of total uptake of AA at 37°C and passive uptake of AA at 4°C. [^{14}C] AA uptake in MDA-MB231 cells was found to be concentration-dependent and saturable with K_m and V_{max} values of 53.85±6.24 μM and 18.45±0.50 pmol/mg protein/min, respectively (Fig. 7A). The kinetic parameters (K_m and V_{max}) estimated for T47D and ZR-75-1 cells were also concentration dependent and saturable with a relatively lower K_m and higher V_{max} than MDA-MB231 cells. K_m and V_{max} values obtained from the saturation kinetics plot for T47D cells were 49.69±2.83 μM and 32.50±0.43pmol/mg protein/min (Fig. 7B), and for ZR-75-1 cell were 45.44±3.16 μM and 33.25±0.53 pmol/mg protein/min respectively (Fig. 7C). Lineweaver-Burk (1/v vs. 1/[S]) plot, indicate the involvement of a single carrier in the uptake process of AA across these breast cancer cell lines (Fig. 7D). Due to nearly similar AA uptake values in T47D and ZR-75-1 cells, overlap of data points was observed in Lineweaver-Burk plot of both the cell lines.

4.4. Role of metabolic and membrane transport inhibitors

Uptake studies were carried out in the presence of metabolic inhibitors such as ouabain (Na^+/K^+ ATPase inhibitor), sodium azide (oxidative phosphorylation inhibitor), and 2,4-DNP (intracellular ATP reducer) in MDA-MB231, T47D and ZR-75-1 cells to delineate the effect of metabolic inhibitors on [^{14}C] AA uptake. These metabolic inhibitors caused significant reduction (50% to 60%) in the uptake of [^{14}C] AA was observed (Fig. 8).

Additional studies were carried out to investigate the effect of membrane inhibitors (SITC, DIDS and probenecid). AA uptake was also reduced to 35% to 45% in the presence of SITC, DIDS and probenecid, suggesting a role of an anion exchanger in carrier mediated transport of [^{14}C] AA (Fig. 9).

4.5. Substrate specificity

[^{14}C] AA uptake in these breast cancer cells was significantly inhibited in the presence of increasing concentration (500, 1000 and 2000μM) of structural analogs (L-AA and D-Iso AA) whereas no substantial alteration in the uptake was observed with DHAA. Also, presence of structurally unrelated analogs i.e. glucose and PAHA (500, 1000 and 2000μM) did not change the uptake of [^{14}C] AA significantly (Fig. 10).

4.6. Intracellular regulation

The role of different intracellular regulation pathways on [^{14}C] AA uptake was also investigated. With higher concentrations of calmidazolium and KN-62 (modulators of Ca^{++}/calmodium (Ca^{++}/CaM) pathway), significantly reduced uptake of [^{14}C] AA was observed in breast cancer cells. PKC activator, PMA (10–100 μM) also caused significant inhibition of AA uptake in all breast cancer cell lines. Inhibitory effect of PMA was muted by BIS (25–100 μM) across all breast cancer cells (Table 1).

Involvement of a PKA-mediated pathway in the regulation of [^{14}C] AA uptake was examined by evaluating the effects of substrates at various concentrations. These compounds are known to induce intracellular cAMP levels (IBMX and forskolin) thus activating PKA in these cells. Concentration dependent effect on the reduction of [^{14}C] AA uptake was evident with IBMX and forskolin, indicating the involvement of cAMP regulated PKA pathways in AA transport. Similarly, we examined the contribution of the PTK pathway on [^{14}C] AA uptake by incubating cells with genistein and tyrphostinA25 for 1 hour. Significantly diminished uptake was observed in the presence of genistein and tyrphostinA25 (modulators of PTK-mediated pathway) across these cell lines (Table 1).

4.7. Reverse Transcription–Polymerase Chain Reaction Analysis

RT-PCR analysis was carried out for the confirmation of AA transport system (SVCT2) in all three breast cancer cell lines. Agarose gel electrophoresis using ethidium bromide was employed to analyze the PCR product. PCR amplification of cDNA from total RNA was performed with a set of primers specific for a human SVCT2 system. The PCR product obtained at 626 bp confirms the expression of the AA transport system (SVCT2) on MDA-MB231, T47D and ZR-75-1 cells. Higher intensity of 626 bp was detected in ZR-75-1 and T47D cell lines relative to MDA-MB231 cells (Fig. 11A). Expression of SVCT2 in breast

tumor cell lines/samples has been significantly associated with ER (estrogen receptor)/PR (progesterone receptor). Greater than 60% of SVCT2 expressing cells demonstrates ER/PR negative, to which the orthodox chemotherapy is usually applied instead of using herceptin, which is efficiently employed for ER/PR-positive breast cancer patients. This finding suggests the potential of vitamin C therapy for breast cancer patients that are ER/PR-negative (Hong et al., 2013). β-Actin was used as internal standard. A 351 base pair band was detected in all the cell lines tested (Fig. 11B).

4.8. Quantitative Real-Time PCR Analysis

Quantitative estimates of the relative abundance of SVCT2 mRNA were obtained with qPCR analysis. mRNA levels of SVCT2 were also analyzed in MDA-MB231, T47D and ZR-75-1 cells. Average C_t values for SVCT2 were around 38–42 and the average C_t values for GAPDH were observed to be 16–19. Significantly higher expression of SVCT2 mRNA in T47D and ZR-75-1 cells was observed relative to MDA-MB231 cells (Fig. 11C).

5. Discussion

AA (vitamin C) is a vital cellular nutrient responsible for normal metabolic and physiological functions. Due to biosynthetic limitation, distribution of AA between extra- and intra-cellular fluids in cells is highly dependent on absorption through functional vitamin C transporters (Savini et al., 2008). Due to its antioxidant nature causing neutralization of free radicals, AA has been postulated to inhibit cancer initiation and promotion (Harris et al., 2013). Several reports have suggested the cytotoxic action of vitamin C against cancer cells (Chen et al., 2008; Ullah et al., 2011). Also, the evidence from various epidemiologic studies cited the role of vitamin C as controversial in breast cancer (Harris et al., 2013). All these biological progressions put emphasis on having a thorough understanding of the mechanism of AA transport in breast cancer cell lines. The main goal of this study was to investigate the functional and molecular expression of SVCT2 in human derived breast cancer cells (MDA-MB231, T47D and ZR-75-1). We have selected these cell lines as an *in vitro* cell culture model because of their aggressive phenotype (Ait-Mohamed et al., 2011; Holliday and Speirs, 2011). Hence, in this study we have investigated the functional and molecular aspects of carrier mediated system responsible for AA uptake on these breast carcinoma cells. Another purpose was to delineate the mechanism of uptake and intracellular regulation.

Since time course of AA uptake showed the linear uptake till 60 min, an incubation time of 30 min was selected for all AA uptake studies in MDA-MB231, T47D and ZR-75-1 cells (Fig. 1). AA uptake appears to be temperature dependent with significant rapid rate at physiological temperature (37°C) relative to 25°C and 4°C (Figs. 2 & 3). Rise in pH resulted in enhanced AA uptake (Figs. 4). Since the $pKa_{1\ of}$ AA is 4.17, it exists primarily in ascorbate form (−1 charge) above the pH 5.0. As a consequence, enhanced AA uptake observed with rise in pH may not be due to the ionic state of AA. It can be concluded from pH dependency results that SVCT2 shows higher affinity towards ascorbate at higher pH (Fig. 4) (Liang et al., 2001; Tsukaguchi et al., 1999). The major forces between SVCT2 and its substrates, responsible for the binding of SVCT2 with the ionized form of AA are ion–

ion and/or ion–polarity interactions. At lower pH, protonation of histidine residues reduces the binding affinity of SVCT2 (Liang et al., 2001).

In the absence of sodium and chloride ions, lower AA uptake was noticed confirming that SVCT2 transporter system may be highly sodium and chloride dependent (Fig. 5A). Additionally, significant inhibition to AA uptake was observed in the presence of amiloride (a Na^+ transport inhibitor) demonstrating that the transport system is highly sodium dependent (Fig. 5A). Transmembrane sodium gradient as well as the membrane potential are responsible for the uphill transport of SVCT2 substrates (Talluri et al., 2006). Therefore, we studied whether the carrier mediated transport via SVCT2 is coupled with the electrochemical gradient of Na^+ ions in MDA-MB231, T47D and ZR-75-1 cells. In all these breast cancer cell lines, diminished uptake of AA was observed with decreasing concentrations of Na^+ in the uptake buffer and was found to be saturated at higher concentrations. These results suggest that AA is coupled to Na^+ and transported directly via SVCT2 (Fig. 5B). The Hill ratio analysis indicates that approximately two sodium ions (1.90 for MDA-MB231, 2.05 for T47D and 2.27 for ZR-75-1) are required for translocation of each AA molecule (Fig. 6).

Concentration dependent uptake of AA clearly reveals that a carrier mediated saturable process is present. In order to distinguish the passive diffusion component from the active AA transport, uptake study was carried out at 4°C in all the breast carcinoma cells. [^{14}C] AA uptake at 4°C was significantly lower than that at 37°C. This suggest the involvement of passive diffusion of AA in these cell lines. AA uptake was found to be saturable with K_m values of 53.85±6.24, 49.69±2.83 and 45.44±3.16 μM and V_{max} values of 18.45±0.50, 32.50±0.43 and 33.25±0.53 pmol/mg protein/min in MDA-MB231, T47D and ZR-75-1 cells, respectively (Figs. 7A, 7B & 7C). Michaelis-Menten kinetic parameters (K_m and V_{max}) are two vital parameters accountable for functional and kinetic constants of a transporter. K_m defines the measure of apparent binding affinity of a substrate whereas V_{max} represents a measure of translocation capacity of the carrier-mediated process. On the basis of Michaelis-Menten kinetics, the K_m value of SVCT2 was found to be higher in MDA-MB231 in comparison to T47D and ZR-75-1 cells, indicating a higher binding strength and affinity of AA for MDA-MB231 cells. The difference in the K_m values observed in MDA-MB231, T47D and ZR-75-1 cells suggested is due to the difference in affinity of ascorbic acid in different cell lines. However, exact mechanism behind different affinity of ascorbic acid for SVCT2 in three different cell lines further investigation in order to delineate the interaction of ascorbic acid at different binding sites of SVCT2. Investigation on the binding sites of SVCT2 with its substrates will be challenging due to the lack of 3D structure of SVCT2 at this time. However comparison of V_{max} values of SVCT2 suggest that transport capacity of SVCT2 in T47D and ZR-75-1 is higher relative to MDA-MB231 cells (32.50±0.43 and 33.25±0.53 vs 18.45±0.50 pmol/mg protein/min). Catalytic efficiency of SVCT2 was estimated by the ratio of Michaelis- Menten kinetic parameters (V_{max}/K_m). A variation in V_{max} values results in higher transport efficiency (V_{max}/K_m) of SVCT2 for T47D and ZR-75-1 (0.65 and 0.73 μl/mg protein/min, respectively) than MDA-MB231 (0.34 μl/mg protein/min). These kinetic parameters indicate possible involvement of a carrier mediated transport system for the translocation of AA in MDA-MB231, T47D and ZR-75-1 cell lines. When the kinetic data was plotted in the form of Lineweaver-Burk (1/v vs. 1/[S])

plot, a single line was obtained for MDA-MB231, T47D and ZR-75-1 cells respectively, which suggests possible involvement of a single transporter for the translocation of AA across breast carcinoma cells (Fig. 7D). Due to nearly similar AA uptake values in T47D and ZR-75-1 cells, overlap of data points was observed in Lineweaver-Burk plot of both the cell lines. These Michaelis-Menten kinetic parameters of SVCT2 in MDA-MB231, T47D and ZR-75-1 cells were in accordance with previously published reports showing the presence of SVCT2 across human retinal cells (Manfredini et al., 2002).

AA uptake was significantly inhibited in all breast cancer cells in the presence of metabolic inhibitors such as sodium azide (oxidative phosphorylation inhibitor), 2,4-dinitrophenol (intracellular ATP reducer) and ouabain, (a known Na+/K+ ATPase inhibitor). This result suggest that uptake of AA via SVCT2 is highly dependent on energy and directly coupled to ATP energy sources (Fig. 8). Uptake of AA was also significantly inhibited in the presence of various membrane/anion inhibitors such as DIDS, SITC, and probenecid (Fig. 9). Similar reports involving inhibition of AA uptake by membrane inhibitors has been published (Dixon et al., 1991; Luo et al., 2008). These results suggest that AA uptake is altered by the presence of specific anions and the site of the SVCT2 transport system may be the plasma membrane (Dixon et al., 1991; Luo et al., 2008).

In MDA-MB231, T47D and ZR-75-1 cells, concentration dependent inhibition of AA uptake mediated via SVCT2 was evident in the presence of structural analogs of AA (L-AA and D-Iso AA). No statistically significant inhibition in the AA uptake via SVCT2 was found in the presence of DHAA (structural analog and GLUT substrate), glucose (GLUT substrate) and PAHA (OAT substrate) (Fig. 10). Similar results with respect to substrate specificity have been reported previously from our laboratory (Katragadda et al., 2005; Luo et al., 2008). Due to a lack of 3D structure of SVCT2 transporter, it is difficult to postulate about structural requirements for the binding of SVCT2 with its substrates and further investigations are required to address the issue.

Several intracellular regulatory pathways such as Ca^{++}/calmodulin, PKA, PTK and PKC are known to be involved in the regulation of AA transport system (Luo et al., 2008). Five putative PKC phosphorylation sites in hSVCT1 and hSVCT2 and one additional PKA site in hSVCT1 have been identified based on the analysis of primary amino acid sequence of SVCT (Liang et al., 2001). It has also been reported that AA uptake by SVCT2 expressed in COS-1 and MDCK-MDR1 cells was under the regulation of PKC-mediated pathway (Liang et al., 2002; Luo et al., 2008). For the same reason, we investigated the regulation of AA uptake by inter- and intra-cellular protein kinase-mediated pathways. Significant inhibition of AA uptake in the presence of calmidazolium and KN-62 was observed in these cell lines suggesting that the AA uptake process is under the regulation of Ca^{++}/CaM mediated pathway. Cell treatment with PMA led to a significant lowering in AA uptake, indicating the role of PKC-mediated pathway on the regulation of AA uptake. Conversely, addition of BIS (PKC pathway inhibitor) reverses the inhibitory effect of PMA signifying the contribution of PKC pathway in controlling this uptake process (Table.1).

On the other hand, significant inhibition on AA uptake by IBMX and forskolin treated breast cancer cells confirms that PKA-mediated pathway plays a vital role in SVCT2 mediated.

Significant inhibition was observed in presence of genistein and tyrphostin A25 (PTK pathway modulators) showing a possible role of PTK pathway in intracellular regulation of AA (Table. 1). Molecular mechanism by which the protein kinase and calmodulin pathway exert their effect on AA uptake process is yet to be fully delineated. Finally, RT-PCR analysis confirms the molecular evidence of a vitamin C/AA specific carrier system in MDA-MB231, T47D and ZR-75-1 cells. An expression of SVCT2 on breast carcinoma cell lines were verified by a specific primer set for the gene. The expression was confirmed by the presence of strong bands of desired size. The PCR product obtained at 626 bp is specific for the SVCT2 transporter system (Fig. 11A). There was a non-specific band of a slightly lower molecular weight observed in the primer set for T47D. qPCR analysis revealed that the expression of SVCT2 was significantly higher in T47D and ZR-75-1 cells in comparison to MDA-MB231 cells (Fig. 11C).

In summary, this work clearly delineates the functional activity and molecular evidence as well as the expression, contribution, and regulation of the sodium-dependent vitamin C transporter 2 (SVCT2) across MDA-MB231, T47D and ZR-75-1 cell lines. AA uptake across MDA-MB231, T47D and ZR-75-1 cells involves a carrier-mediated active process which is controlled by both Ca^{++}/CaM mediated as well as protein kinases pathways. This transporter is highly pH dependent and requires coupling to an electrochemical Na^{+} gradient and ATP sources for cellular uptake. This membrane transporter (SVCT2) can be utilized as a potential target for enhancing permeability and bioavailability of highly potent anti-cancer drugs. Our investigation demonstrates complete profiling of SVCT2 mediated AA uptake and its dependence on calmodulin, protein kinases and intracellular ions. Demarcation of AA uptake and transport mechanism by SVCT2 can aid in achieving therapeutic drug concentrations at the target site. The results may help in providing cancer chemotherapy by evasion of efflux pumps in cancer cells and overcoming chemotherapeutic resistance which is an obstacle in the treatment of breast cancer. Also, MDA-MB231, T47D and ZR-75-1 cell lines can be utilized as a valuable *in vitro* model to investigate absorption and permeability of AA-conjugated chemotherapeutics.

Acknowledgments

This work was supported by National Institutes of Health grant 1R01 AI071199. The authors highly appreciate Dr. Walter Jäger University of Vienna, Austria) and Dr. A.J. van Agthoven (Josephine Nefkens Institute, Netherlands) for their generous gift of MDA-MB231 and ZR-75-1 cell lines.

References

Ait-Mohamed O, Battisti V, Joliot V, Fritsch L, Pontis J, Medjkane S, Redeuilh C, Lamouri A, Fahy C, Rholam M, Atmani D, Ait-Si-Ali S. Acetonic extract of Buxus sempervirens induces cell cycle arrest, apoptosis and autophagy in breast cancer cells. PloS one. 2011; 6:e24537. [PubMed: 21935420]

Baader SL, Bill E, Trautwein AX, Bruchelt G, Matzanke BF. Mobilization of iron from cellular ferritin by ascorbic acid in neuroblastoma SK-N-SH cells: an EPR study. FEBS letters. 1996; 381:131–134. [PubMed: 8641421]

Bareford LM, Phelps MA, Foraker AB, Swaan PW. Intracellular processing of riboflavin in human breast cancer cells. Molecular pharmaceutics. 2008; 5:839–848. [PubMed: 18754669]

Bowers-Komro DM, McCormick DB. Characterization of ascorbic acid uptake by isolated rat kidney cells. J Nutr. 1991; 121:57–64. [PubMed: 1992058]

Burzle M, Suzuki Y, Ackermann D, Miyazaki H, Maeda N, Clemencon B, Burrier R, Hediger MA. The sodium-dependent ascorbic acid transporter family SLC23. Molecular aspects of medicine. 2013; 34:436–454. [PubMed: 23506882]

Cameron E, Campbell A. The orthomolecular treatment of cancer. II. Clinical trial of high-dose ascorbic acid supplements in advanced human cancer. Chemico-biological interactions. 1974; 9:285–315. [PubMed: 4430016]

Cameron E, Pauling L. Supplemental ascorbate in the supportive treatment of cancer: Prolongation of survival times in terminal human cancer. Proceedings of the National Academy of Sciences of the United States of America. 1976; 73:3685–3689. [PubMed: 1068480]

Cameron E, Pauling L. Supplemental ascorbate in the supportive treatment of cancer: reevaluation of prolongation of survival times in terminal human cancer. Proceedings of the National Academy of Sciences of the United States of America. 1978; 75:4538–4542. [PubMed: 279931]

Castro M, Caprile T, Astuya A, Millan C, Reinicke K, Vera JC, Vasquez O, Aguayo LG, Nualart F. High-affinity sodium-vitamin C co-transporters (SVCT) expression in embryonic mouse neurons. J Neurochem. 2001; 78:815–823. [PubMed: 11520902]

Chen Q, Espey MG, Sun AY, Pooput C, Kirk KL, Krishna MC, Khosh DB, Drisko J, Levine M. Pharmacologic doses of ascorbate act as a prooxidant and decrease growth of aggressive tumor xenografts in mice. Proceedings of the National Academy of Sciences of the United States of America. 2008; 105:11105–11109. [PubMed: 18678913]

Cole SP, Bhardwaj G, Gerlach JH, Mackie JE, Grant CE, Almquist KC, Stewart AJ, Kurz EU, Duncan AM, Deeley RG. Overexpression of a transporter gene in a multidrug-resistant human lung cancer cell line. Science. 1992; 258:1650–1654. [PubMed: 1360704]

Constable PA, Lawrenson JG, Dolman DE, Arden GB, Abbott NJ. P-Glycoprotein expression in human retinal pigment epithelium cell lines. Experimental eye research. 2006; 83:24–30. [PubMed: 16530756]

Davis AA, Bernstein PS, Bok D, Turner J, Nachtigal M, Hunt RC. A human retinal pigment epithelial cell line that retains epithelial characteristics after prolonged culture. Investigative ophthalmology & visual science. 1995; 36:955–964. [PubMed: 7706045]

Dixon SJ, Kulaga A, Jaworski EM, Wilson JX. Ascorbate uptake by ROS 17/2.8 osteoblast-like cells: substrate specificity and sensitivity to transport inhibitors. J Bone Miner Res. 1991; 6:623–629. [PubMed: 1887825]

Doyle LA, Yang W, Abruzzo LV, Krogmann T, Gao Y, Rishi AK, Ross DD. A multidrug resistance transporter from human MCF-7 breast cancer cells. Proceedings of the National Academy of Sciences of the United States of America. 1998; 95:15665–15670. [PubMed: 9861027]

Gallagher SM, Castorino JJ, Wang D, Philp NJ. Monocarboxylate transporter 4 regulates maturation and trafficking of CD147 to the plasma membrane in the metastatic breast cancer cell line MDA-MB-231. Cancer research. 2007; 67:4182–4189. [PubMed: 17483329]

Garland DL. Ascorbic acid and the eye. Am J Clin Nutr. 1991; 54:1198S–1202S. [PubMed: 1962570]

Gros P, Ben Neriah YB, Croop JM, Housman DE. Isolation and expression of a complementary DNA that confers multidrug resistance. Nature. 1986; 323:728–731. [PubMed: 3022150]

Harris HR, Bergkvist L, Wolk A. Vitamin C intake and breast cancer mortality in a cohort of Swedish women. British journal of cancer. 2013; 109:257–264. [PubMed: 23736027]

Harris T, Eliyahu G, Frydman L, Degani H. Kinetics of hyperpolarized 13C1-pyruvate transport and metabolism in living human breast cancer cells. Proceedings of the National Academy of Sciences of the United States of America. 2009; 106:18131–18136. [PubMed: 19826085]

Head KA. Ascorbic acid in the prevention and treatment of cancer. Alternative medicine review: a journal of clinical therapeutic. 1998; 3:174–186. [PubMed: 9630735]

Holliday DL, Speirs V. Choosing the right cell line for breast cancer research. Breast cancer research: BCR. 2011; 13:215. [PubMed: 21884641]

Hong SW, Lee SH, Moon JH, Hwang JJ, Kim DE, Ko E, Kim HS, Cho IJ, Kang JS, Kim DJ, Kim JE, Shin JS, Jung DJ, Jeong YJ, Cho BJ, Kim TW, Lee JS, Kang JS, Hwang YI, Noh DY, Jin DH, Lee WJ. SVCT-2 in breast cancer acts as an indicator for L-ascorbate treatment. Oncogene. 2013; 32:1508–1517. [PubMed: 22665050]

Jhaveri MS, Rait AS, Chung KN, Trepel JB, Chang EH. Antisense oligonucleotides targeted to the human alpha folate receptor inhibit breast cancer cell growth and sensitize the cells to doxorubicin treatment. Molecular cancer therapeutics. 2004; 3:1505–1512. [PubMed: 15634643]

Kang JS, Cho D, Kim YI, Hahm E, Kim YS, Jin SN, Kim HN, Kim D, Hur D, Park H, Hwang YI, Lee WJ. Sodium ascorbate (vitamin C) induces apoptosis in melanoma cells via the down-regulation of transferrin receptor dependent iron uptake. Journal of cellular physiology. 2005; 204:192–197. [PubMed: 15672419]

Katragadda S, Talluri RS, Pal D, Mitra AK. Identification and characterization of a Na+-dependent neutral amino acid transporter, ASCT1, in rabbit corneal epithelial cell culture and rabbit cornea. Curr Eye Res. 2005; 30:989–1002. [PubMed: 16282133]

Kessel D, Botterill V, Wodinsky I. Uptake and retention of daunomycin by mouse leukemic cells as factors in drug response. Cancer research. 1968; 28:938–941. [PubMed: 5652307]

Khurana V, Minocha M, Pal D, Mitra AK. Inhibition of OATP-1B1 and OATP-1B3 by tyrosine kinase inhibitors. Drug metabolism and drug interactions. 2014a

Khurana V, Minocha M, Pal D, Mitra AK. Role of OATP-1B1 and/or OATP-1B3 in hepatic disposition of tyrosine kinase inhibitors. Drug metabolism and drug interactions. 2014b

Kurbacher CM, Wagner U, Kolster B, Andreotti PE, Krebs D, Bruckner HW. Ascorbic acid (vitamin C) improves the antineoplastic activity of doxorubicin, cisplatin, and paclitaxel in human breast carcinoma cells in vitro. Cancer letters. 1996; 103:183–189. [PubMed: 8635156]

Liang WJ, Johnson D, Jarvis SM. Vitamin C transport systems of mammalian cells. Mol Membr Biol. 2001; 18:87–95. [PubMed: 11396616]

Liang WJ, Johnson D, Ma LS, Jarvis SM, Wei-Jun L. Regulation of the human vitamin C transporters expressed in COS-1 cells by protein kinase C [corrected]. American journal of physiology. Cell physiology. 2002; 283:C1696–1704. [PubMed: 12388072]

Ling V, Thompson LH. Reduced permeability in CHO cells as a mechanism of resistance to colchicine. Journal of cellular physiology. 1974; 83:103–116. [PubMed: 4855907]

Luo S, Wang Z, Kansara V, Pal D, Mitra AK. Activity of a sodium-dependent vitamin C transporter (SVCT) in MDCK-MDR1 cells and mechanism of ascorbate uptake. International journal of pharmaceutics. 2008; 358:168–176. [PubMed: 18417304]

Luo S, Wang Z, Patel M, Khurana V, Zhu X, Pal D, Mitra AK. Targeting SVCT for enhanced drug absorption: synthesis and in vitro evaluation of a novel vitamin C conjugated prodrug of saquinavir. International journal of pharmaceutics. 2011; 414:77–85. [PubMed: 21571053]

Manfredini S, Pavan B, Vertuani S, Scaglianti M, Compagnone D, Biondi C, Scatturin A, Tanganelli S, Ferraro L, Prasad P, Dalpiaz A. Design, synthesis and activity of ascorbic acid prodrugs of nipecotic, kynurenic and diclophenamic acids, liable to increase neurotropic activity. Journal of medicinal chemistry. 2002; 45:559–562. [PubMed: 11806707]

Maramag C, Menon M, Balaji KC, Reddy PG, Laxmanan S. Effect of vitamin C on prostate cancer cells in vitro: effect on cell number, viability, and DNA synthesis. The Prostate. 1997; 32:188–195. [PubMed: 9254898]

Marshman E, Taylor GA, Thomas HD, Newell DR, Curtin NJ. Hypoxanthine transport in human tumour cell lines: relationship to the inhibition of hypoxanthine rescue by dipyridamole. Biochemical pharmacology. 2001; 61:477–484. [PubMed: 11226382]

Maulen NP, Henriquez EA, Kempe S, Carcamo JG, Schmid-Kotsas A, Bachem M, Grunert A, Bustamante ME, Nualart F, Vera JC. Up-regulation and polarized expression of the sodium-ascorbic acid transporter SVCT1 in post-confluent differentiated CaCo-2 cells. The Journal of biological chemistry. 2003; 278:9035–9041. [PubMed: 12381735]

Menniti FS, Knoth J, Diliberto EJ Jr. Role of ascorbic acid in dopamine beta-hydroxylation. The endogenous enzyme cofactor and putative electron donor for cofactor regeneration. The Journal of biological chemistry. 1986; 261:16901–16908. [PubMed: 3097015]

Minocha M, Khurana V, Qin B, Pal D, Mitra AK. Enhanced brain accumulation of pazopanib by modulating P-gp and Bcrp1 mediated efflux with canertinib or erlotinib. International journal of pharmaceutics. 436:127–134. [PubMed: 22688250]

Murad S, Grove D, Lindberg KA, Reynolds G, Sivarajah A, Pinnell SR. Regulation of collagen synthesis by ascorbic acid. Proceedings of the National Academy of Sciences of the United States of America. 1981; 78:2879–2882. [PubMed: 6265920]

Ohno S, Ohno Y, Suzuki N, Soma G, Inoue M. High-dose vitamin C (ascorbic acid) therapy in the treatment of patients with advanced cancer. Anticancer research. 2009; 29:809–815. [PubMed: 19414313]

Okabe M, Szakacs G, Reimers MA, Suzuki T, Hall MD, Abe T, Weinstein JN, Gottesman MM. Profiling SLCO and SLC22 genes in the NCI-60 cancer cell lines to identify drug uptake transporters. Molecular cancer therapeutics. 2008; 7:3081–3091. [PubMed: 18790787]

Padayatty SJ, Levine M. Reevaluation of ascorbate in cancer treatment: emerging evidence, open minds and serendipity. Journal of the American College of Nutrition. 2000; 19:423–425. [PubMed: 10963459]

Padh H, Aleo JJ. Characterization of the ascorbic acid transport by 3T6 fibroblasts. Biochimica et biophysica acta. 1987; 901:283–290. [PubMed: 3607050]

Patak P, Willenberg HS, Bornstein SR. Vitamin C is an important cofactor for both adrenal cortex and adrenal medulla. Endocrine research. 2004; 30:871–875. [PubMed: 15666839]

Patel M, Vadlapatla RK, Shah S, Mitra AK. Molecular expression and functional activity of sodium dependent multivitamin transporter in human prostate cancer cells. International journal of pharmaceutics. 2012; 436:324–331. [PubMed: 22732670]

Pfaffl MW. A new mathematical model for relative quantification in real-time RT-PCR. Nucleic acids research. 2001; 29:e45. [PubMed: 11328886]

Pinard MF, Jolivet J, Ratnam M, Kathmann I, Molthoff C, Westerhof R, Schornagel JH, Jansen G. Functional aspects of membrane folate receptors in human breast cancer cells with transport-related resistance to methotrexate. Cancer chemotherapy and pharmacology. 1996; 38:281–288. [PubMed: 8646804]

Plagemann PG, Wohlhueter RM, Woffendin C. Nucleoside and nucleobase transport in animal cells. Biochimica et biophysica acta. 1988; 947:405–443. [PubMed: 3048401]

Riehm H, Biedler JL. Cellular resistance to daunomycin in Chinese hamster cells in vitro. Cancer research. 1971; 31:409–412. [PubMed: 5102828]

Rivenzon-Segal D, Rushkin E, Polak-Charcon S, Degani H. Glucose transporters and transport kinetics in retinoic acid-differentiated T47D human breast cancer cells. American journal of physiology. Endocrinology and metabolism. 2000; 279:E508–519. [PubMed: 10950817]

Savini I, Rossi A, Pierro C, Avigliano L, Catani MV. SVCT1 and SVCT2: key proteins for vitamin C uptake. Amino acids. 2008; 34:347–355. [PubMed: 17541511]

Shennan DB. Mammary gland membrane transport systems. Journal of mammary gland biology and neoplasia. 1998; 3:247–258. [PubMed: 10819512]

Stebbing J, Ellis P. An overview of drug development for metastatic breast cancer. British journal of nursing. 2012; 21:S18–22. [PubMed: 22470903]

Talluri RS, Katragadda S, Pal D, Mitra AK. Mechanism of L-ascorbic acid uptake by rabbit corneal epithelial cells: evidence for the involvement of sodium-dependent vitamin C transporter 2. Curr Eye Res. 2006; 31:481–489. [PubMed: 16769607]

Tamai I. Oral drug delivery utilizing intestinal OATP transporters. Advanced drug delivery reviews. 2012; 64:508–514. [PubMed: 21824501]

Tsukaguchi H, Tokui T, Mackenzie B, Berger UV, Chen XZ, Wang Y, Brubaker RF, Hediger MA. A family of mammalian Na+-dependent L-ascorbic acid transporters. Nature. 1999; 399:70–75. [PubMed: 10331392]

Ullah MF, Khan HY, Zubair H, Shamim U, Hadi SM. The antioxidant ascorbic acid mobilizes nuclear copper leading to a prooxidant breakage of cellular DNA: implications for chemotherapeutic action against cancer. Cancer chemotherapy and pharmacology. 2011; 67:103–110. [PubMed: 20213077]

Vadlapudi AD, Vadlapatla RK, Pal D, Mitra AK. Functional and Molecular Aspects of Biotin Uptake via SMVT in Human Corneal Epithelial (HCEC) and Retinal Pigment Epithelial (D407) Cells. AAPS J. 2012

Vadlapudi AD, Vadlapatla RK, Pal D, Mitra AK. Biotin uptake by T47D breast cancer cells: functional and molecular evidence of sodium-dependent multivitamin transporter (SMVT). International journal of pharmaceutics. 2013; 441:535–543. [PubMed: 23142496]

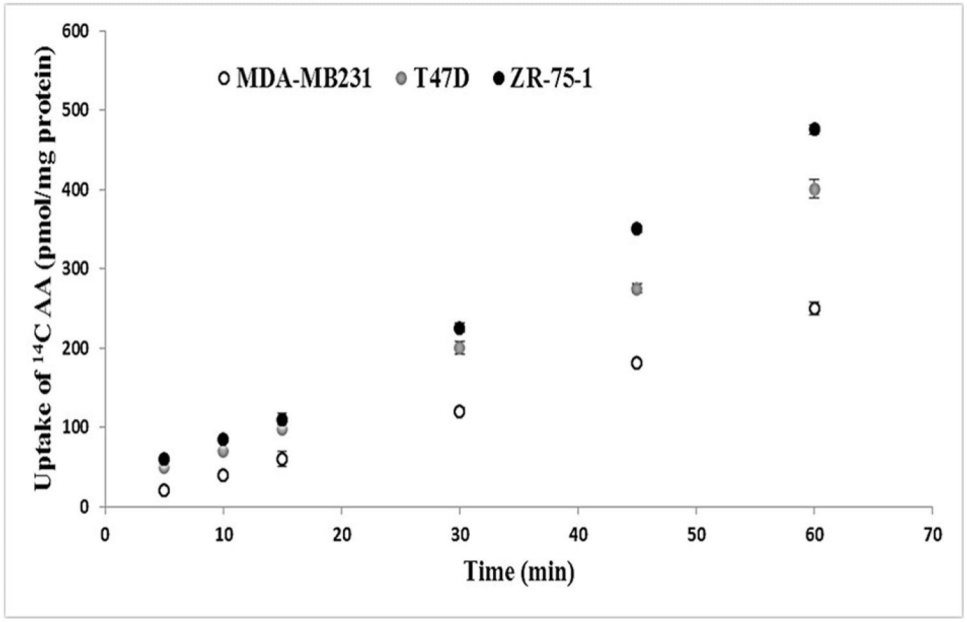

Fig. 1.

Time course of [^{14}C] AA uptake across MDA-MB231, T47D and ZR-75-1 cells. Uptake of [^{14}C] ascorbic acid ([^{14}C] AA) was measured in DPBS buffer (pH 7.4) at 37°C. Data is shown as mean±S.D. n=4. S.D. means standard derivation.

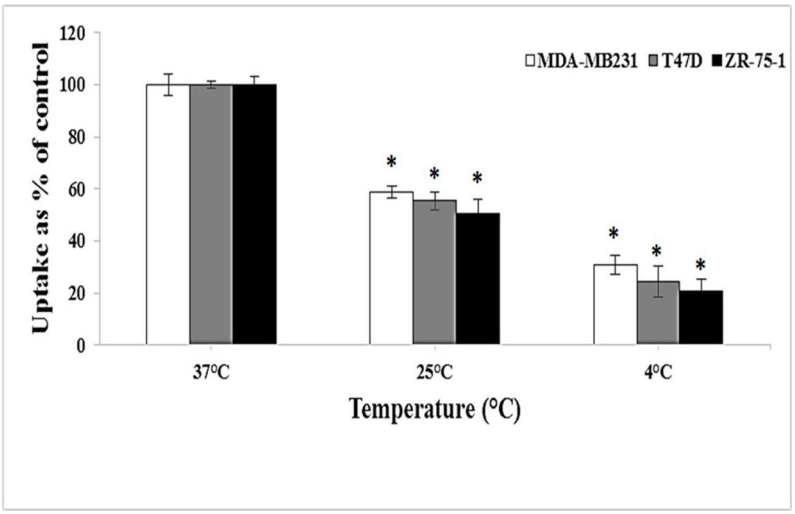

Fig. 2.

Temperature dependent uptake study of [^{14}C] AA uptake across MDA-MB231, T47D and ZR-75-1 cells in DPBS (pH 7.4). The uptake is expressed as percentage of control (37°C). Data is shown as mean±S.D. n=4. Asterisk (*) represents significant difference from the control (*$p<0.05$).

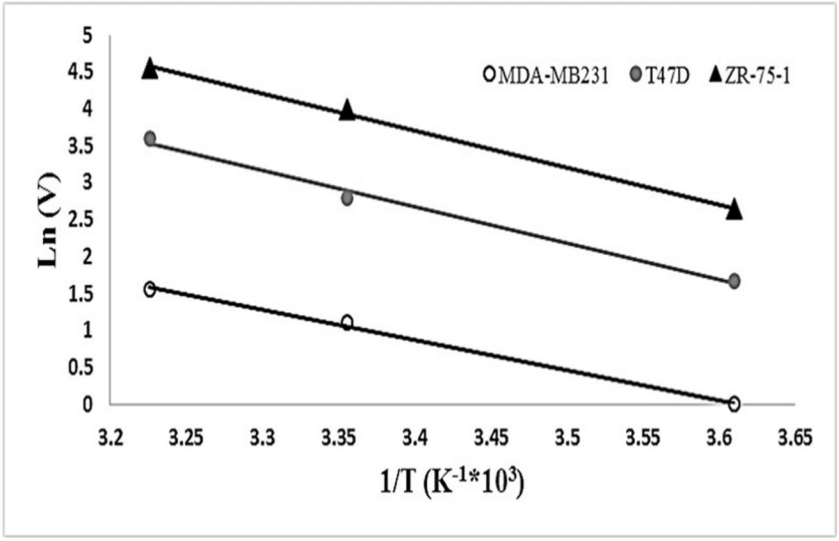

Fig. 3.

Arrhenius plot of the effect of temperature on [^{14}C] AA uptake across MDA-MB231, T47D and ZR-75-1 cells. Uptake of [^{14}C] AA was measured in DPBS buffer (pH 7.4) for 30min at 37, 25 and 4°C, across MDA-MB231, T47D and ZR-75-1 cells. Data is shown as mean ±S.D. n=4

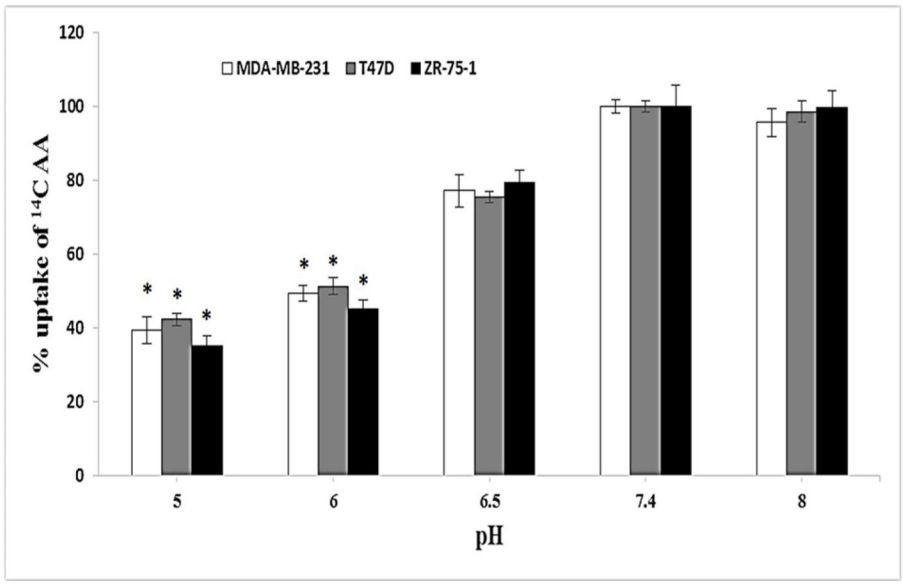

Fig. 4.

Effect of pH on [^{14}C] AA uptake across MDA-MB231, T47D and ZR-75-1 cells. Uptake of [^{14}C] AA was determined in the presence of different pH (5.0, 6.0, 6.5, 7.4 and 8.0) at 37°C for 30 min across MDA-MB231, T47D and ZR-75-1 cells. The uptake is expressed as percentage of control (pH 7.4). Data is shown as mean±S.D. n=4. (*$p<0.05$).

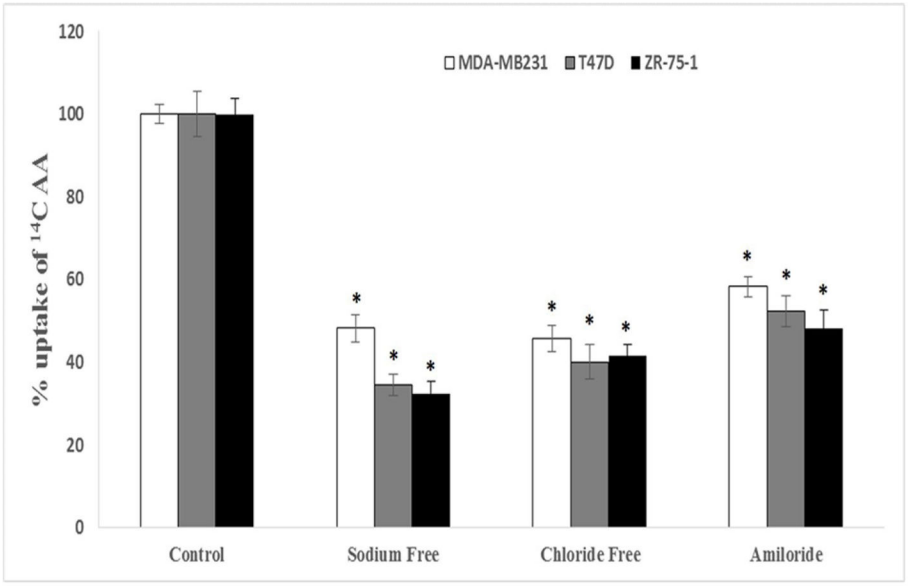

Fig5A .

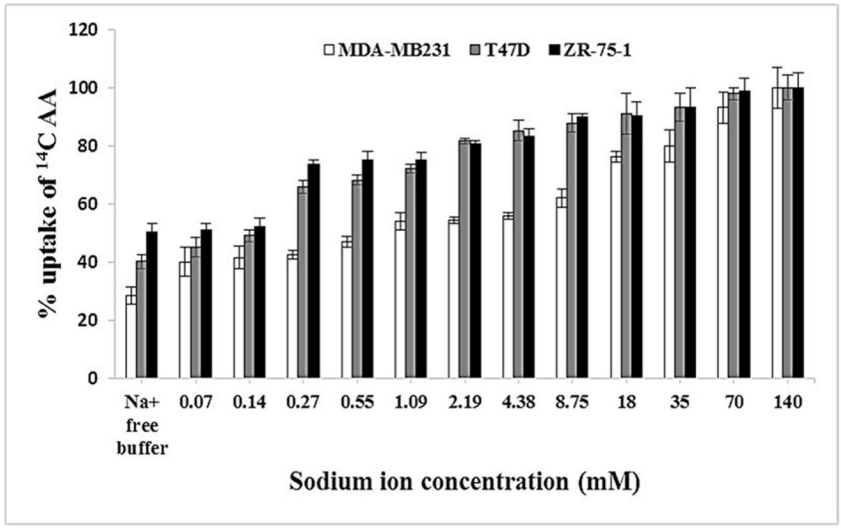

Fig5B .

Fig. 5.

(A) Uptake of [^{14}C] AA across MDA-MB231, T47D and ZR-75-1 cells in the presence of amiloride and absence of sodium and chloride ions in DPBS buffer (pH 7.4) at 37°C. (*$p<0.05$); **(B)** Uptake of [^{14}C] AA across MDA-MB231, T47D and ZR-75-1 cells as a function of sodium concentration in DPBS (pH 7.4) at 37°C. Data is shown as mean±S.D. n=4.

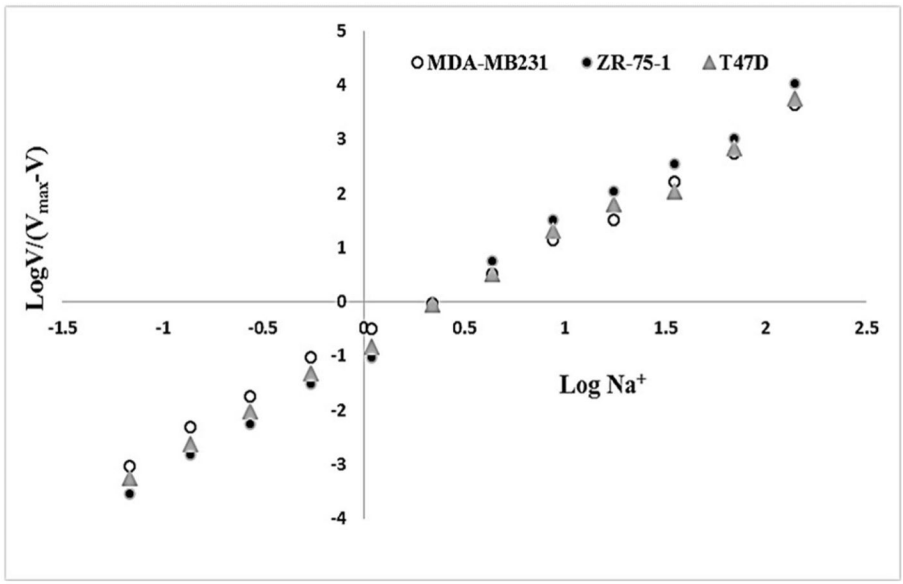

Fig. 6.

Hill plot of sodium-dependent uptake of [^{14}C] AA across MDA-MB231, T47D and ZR-75-1 cells.

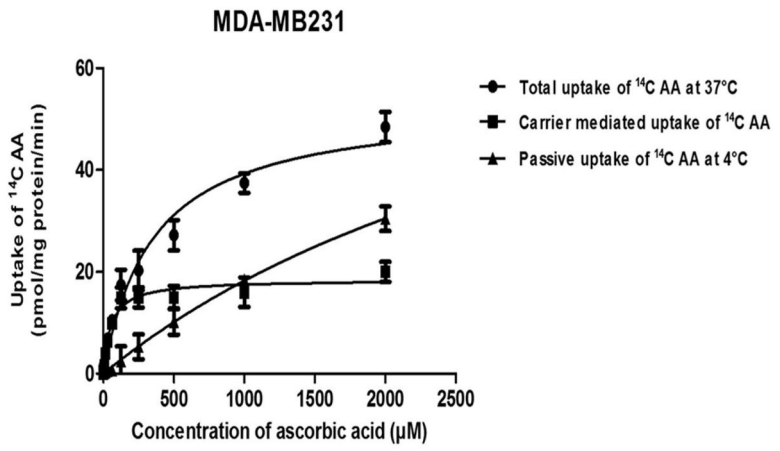

Fig7A .

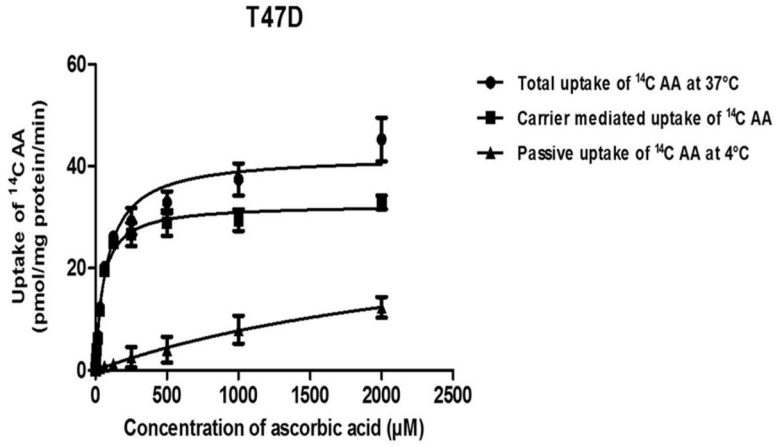

Fig7B .

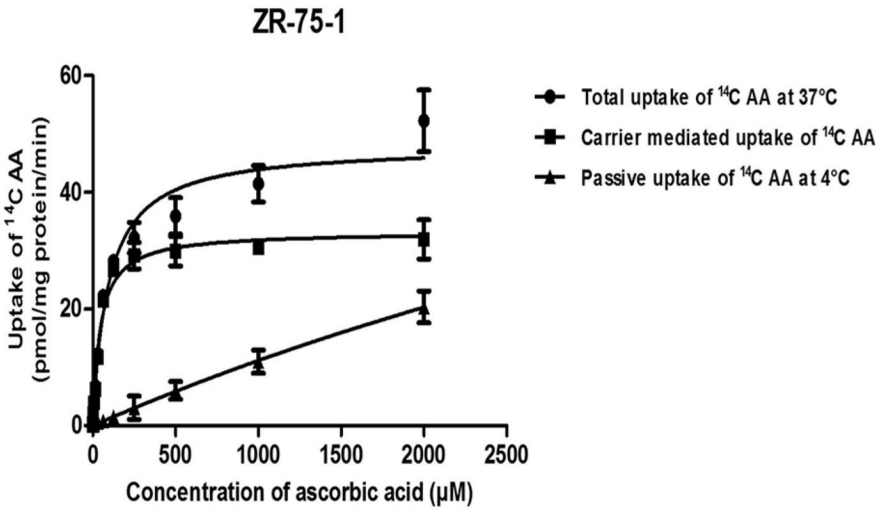

Fig7C .

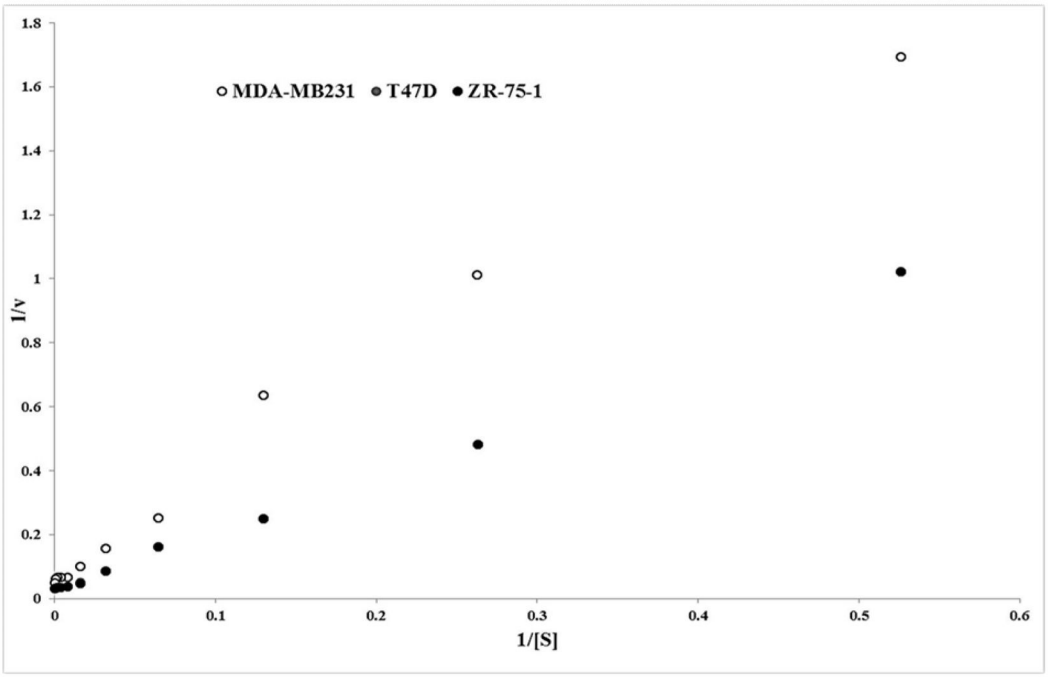

Fig7D .

Fig. 7.

(A) Concentration-dependent uptake of [^{14}C] AA across MDA-MB231 cells. Data is shown as mean±S.D. n=4 (● represents total uptake, ▲ represents passive uptake/non-saturable component and ■ represents carrier mediated uptake/saturable component); **(B)** Concentration-dependent uptake of [^{14}C] AA across T47D cells. Data is shown as mean ±S.D. n=4 (● represents total uptake, ▲ represents passive uptake/non-saturable component and ■ represents carrier mediated uptake/saturable component); **(C)** Concentration-

dependent uptake of [^{14}C] AA across ZR-75-1 cells. Data is shown as mean±S.D. n=4 (● represents total uptake, ▲ represents passive uptake/non-saturable component and ■ represents carrier mediated uptake/saturable component); **(D)** Lineweaver–Burk transformation of the data demonstrated involvement of a single carrier mediated process for the uptake of [^{14}C] AA across MDA-MB231, T47D and ZR-75-1 cells.

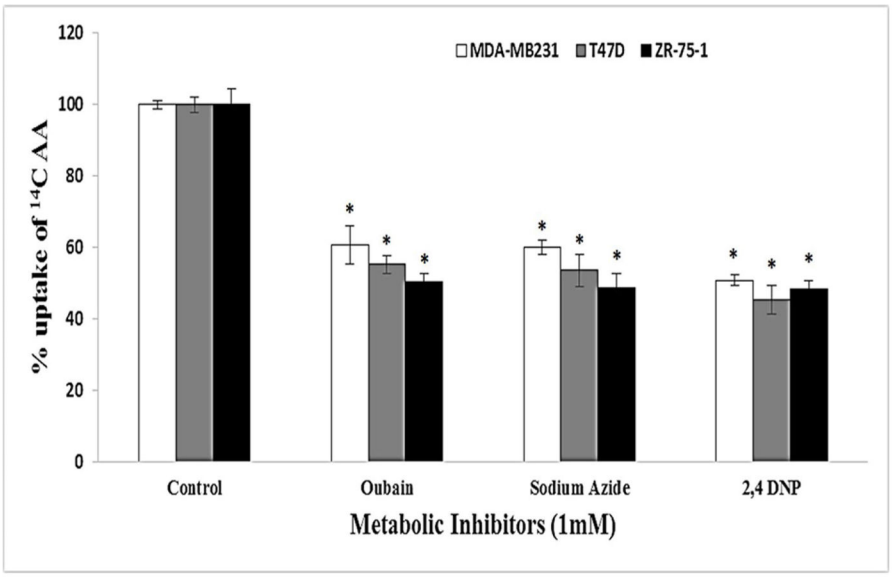

Fig. 8.

Uptake of [^{14}C] AA across MDA-MB231, T47D and ZR-75-1 cells in the presence of metabolic inhibitors (ouabain, sodium azide, and 2,4-DNP). [^{14}C] AA uptake was performed at 37°C with DPBS buffer (pH 7.4) for 30 min. Data is shown as mean±S.D. n=4. (*$p<0.05$).

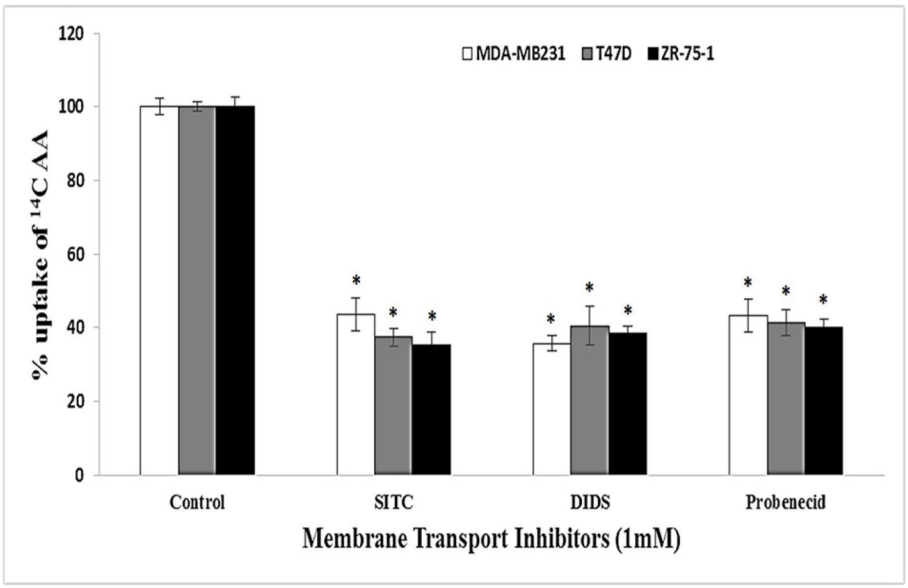

Fig. 9.

Uptake of [^{14}C] AA across MDA-MB231, T47D and ZR-75-1 cells in the presence of membrane inhibitors (SITC, DIDS and probenecid). [^{14}C] AA uptake was performed at 37°C with DPBS buffer (pH 7.4) for 30 min. Data is shown as mean±S.D. n=4. (*$p<0.05$).

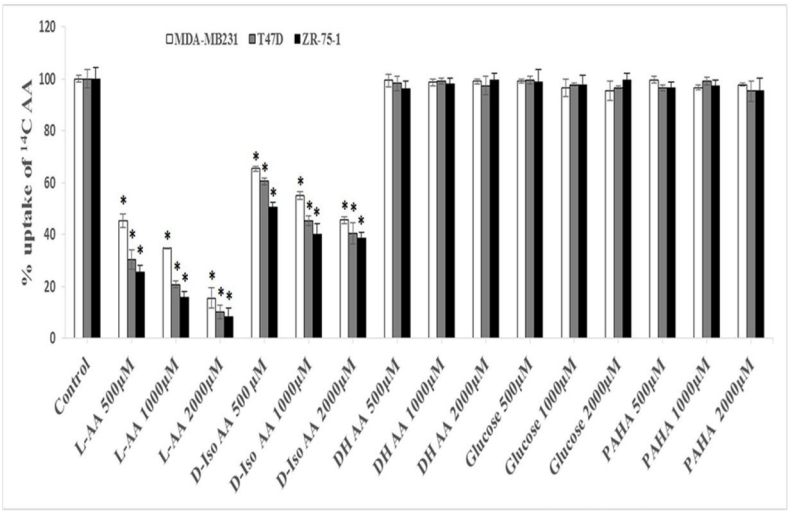

Fig. 10.

Uptake of [^{14}C] AA in presence of L-ascorbic acid (L-AA), D-isoascorbic acid (D-Iso AA), dehydro ascorbic acid (DHAA), D-glucose, and para-amino hippuric acid (PAHA) at three different concentrations across MDA-MB231, T47D and ZR-75-1 cells. [^{14}C] AA uptake was performed at 37°C with DPBS buffer (pH 7.4) for 30 min. Data is shown as mean±S.D. n=4. (*$p<0.05$).

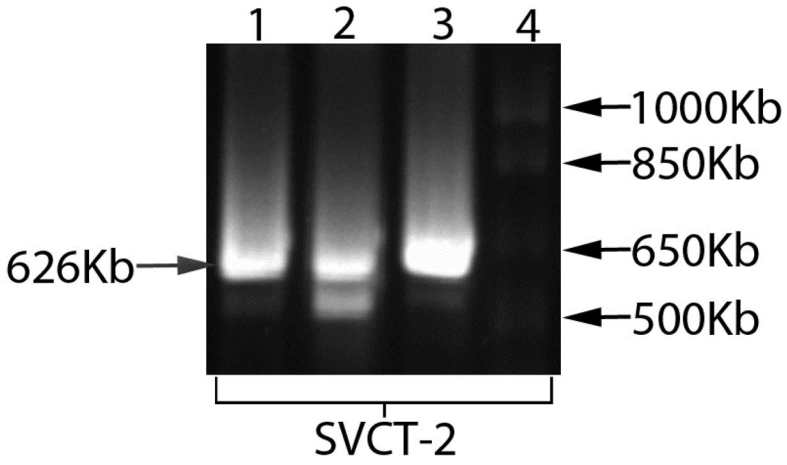

Fig. 11A

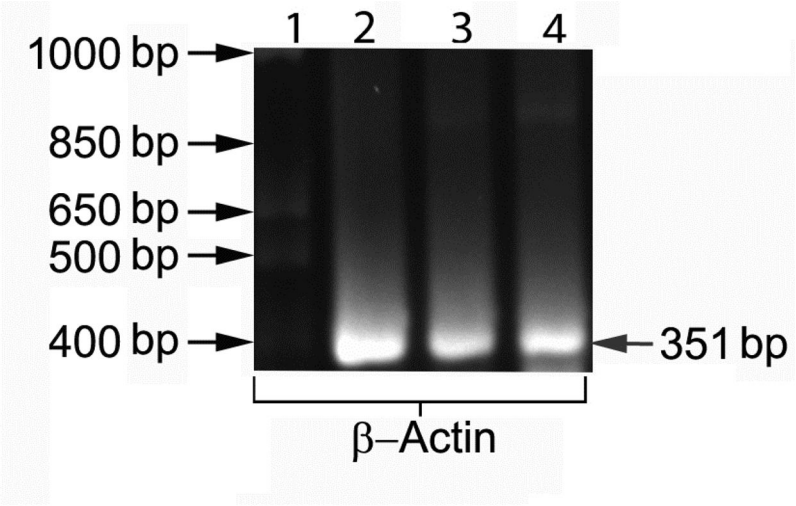

Fig. 11B

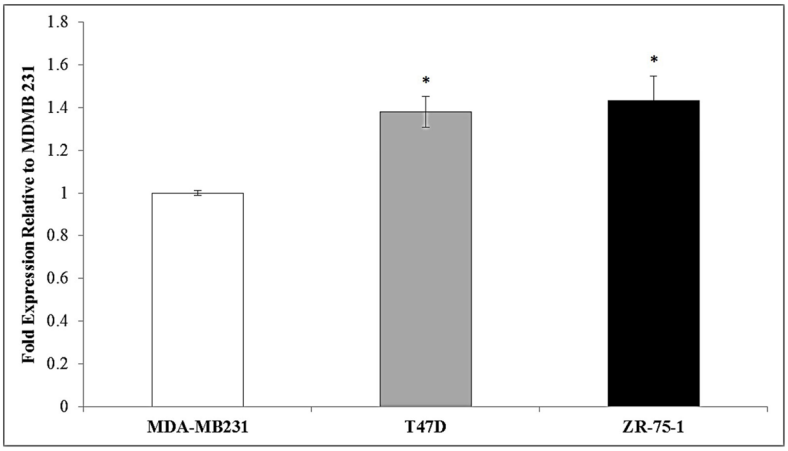

Fig. 11C

Fig. 11.

(A) RT-PCR studies showing the molecular evidence of SVCT2 in MDA-MB231, T47D and ZR-75-1 cells. Lane 1 represents ZR-75-1, lane 2: T47D, lane 3: MDA-MB231 and lane 4: 1 Kb molecular ladder. **(B)** RT-PCR studies showing the molecular evidence of β-actin in in MDA-MB231, T47D and ZR-75-1 cells. Lane 1 represents 1 Kb molecular ladder, lane 2: ZR-75-1, lane 3: T47D and lane 4: MDA-MB231. **(C)** Real time-PCR comparing the expression of SVCT2 in MDA-MB231, T47D and ZR-75-1 cells. Data is shown as mean ±S.D. n=4. (*$p<0.05$).

Table 1

Uptake of [^{14}C] AA across MDA-MB231, T47D and ZR-75-1 cells in the presence of various concentrations of Ca^{++}/calmodulin pathway, PKC pathway, PKA pathway and PTK pathway modulators in DPBS (pH 7.4) at 37 °C. The uptake is expressed as percentage of control (DPBS).

Pathways	Modulators	Uptake as % of Control		
		MDA-MB231	T47D	ZR-75-1
Ca^{++}/calmodulin pathway	Control	100 ± 1.57	100 ± 2.89	100 ± 4.12
	CaM (10μM)	38.55 ± 3.56*	32.89 ± 2.48*	31.49 ± 1.56*
	CaM (50μM)	35.18 ± 2.15*	27.69 ± 4.25*	25.78 ± 3.53*
	CaM (100μM)	24.45 ± 3.18*	18.46± 3.85*	15.63± 2.17*
	KN-62 (0.1μM)	48.68 ± 2.89*	38.14 ± 2.59*	40.14 ± 3.19*
	KN-62 (1μM)	38.45 ± 4.51*	25.91± 4.21*	28.76± 1.05*
	KN-62 (10μM)	25.26 ± 6.72*	21.83± 2.43*	19.45± 2.35*
PKC pathway	Control	100 ± 5.52	100 ± 3.19	100 ± 2.69
	PMA (10μM)	52.35 ± 4.65*	54.82 ± 3.54*	55.46 ± 2.89*
	PMA (50μM)	50.23 ± 2.38*	47.61 ± 2.19*	50.12 ± 3.67*
	PMA (100μM)	44.98 ± 6.34*	40.75 ± 4.85*	42.15 ± 5.48*
	PMA (100μM) + BIS (25μM)	89.23 ± 6.35	90.25 ± 5.92	88.68 ± 7.89
	PMA (100μM) + BIS (50μM)	92.85 ± 4.39	92.68 ± 3.45	93.63 ± 5.67
	PMA (100μM) + BIS (100μM)	95.34 ± 3.48	93.15 ± 4.85	94.19 ± 2.11
PKA pathway	Control	100 ± 3.24	100 ± 2.65	100 ± 6.32
	IBMX (0.1μM)	36.23 ± 4.21*	40.13 ± 4.21*	39.65 ± 2.12*
	IBMX (1μM)	30.64 ± 2.87*	35.84 ± 2.78*	36.48 ± 5.87*
	IBMX (5μM)	25.96 ± 5.12*	32.67 ± 4.51*	30.76 ± 2.15*
	Forskolin (1μM)	33.14 ± 4.29*	38.21 ± 3.53*	40.12 ± 5.33*
	Forkolin (10μM)	30.97 ± 7.19*	32.49 ± 7.89*	38.94 ± 6.98*
	Forskolin (50μM)	25.73 ± 4.28*	31.96 ± 4.56*	35.69 ± 3.65*
	Forskolin (100μM)	22.81 ± 2.16*	25.78 ± 2.55*	30.87 ± 5.22*
PTK pathway	Control	100 ± 5.52	100 ± 3.19	100 ± 2.69
	Genistein (10μM)	52.35 ± 4.65*	54.82 ± 3.54*	55.46 ± 2.89*
	Genistein (50μM)	50.23 ± 2.38*	47.61 ± 2.19*	50.12 ± 3.67*
	Genistein (100μM)	44.98 ± 6.34*	40.75 ± 4.85*	42.15 ± 5.48*
	Tyrphostin A25 (10μM)	54.65 ± 6.35*	50.25 ± 5.92*	48.68 ± 7.89*
	Tyrphostin A25 (50μM)	45.78 ± 4.39*	42.68 ± 3.45*	43.63 ± 5.67*
	Tyrphostin A25 (100μM)	33.21 ± 3.48*	36.15 ± 4.85*	34.19 ± 2.11*

Data is shown as mean±S.D. n=4. (*p<0.05).